ÉCOLE POLYTECHNIQUE
FÉDÉRALE DE LAUSANNE

Nuclear Magnetic Resonance

Jakob Odersky
jakob.odersky@epfl.ch

Simon Löwe
simon.loewe@epfl.ch

November 20, 2012

Contents

1 Introduction

Nuclear Magnetic Resonance (NMR) is a phenomenon in which nuclei start to absorb and re-emit electromagnetic radiation when they are themselves excited under a varying magnetic field. The frequency at which the absorption and emission occur, depends on the charge of the nuclei and the intensity of magnetic field. Considering the first of these dependencies, NMR may be used to determine the composition of an unknown probe (such as in NMR spectroscopy). Furthermore, considering that the resonance frequency of the nuclei also depends on the intensity of the magnetic field, by applying a non-uniform field, NMR may be used as an imaging technique by mapping specific frequencies to points in space (such as in medical magnetic resonance imagery).

This report explores these two applications by determining various characteristics of probes of Cu_2SO_4 of unknown concentrations, and by reconstituting images of teflon shapes in a solution.

2 Theory

Nuclear Magnetic Resonance (short NMR) is an inherently quantum mechanical phenomenon. The basic properties of NMR-spectroscopy which will be studied in this experiment can be understood by a classical approach, if one accepts that the nucleus of an atom has two new properties:

1. The nucleus has an angular momentum $\boldsymbol{j}$
2. The nucleus has a magnetic moment, called spin, given by $\boldsymbol{m} = \gamma \boldsymbol{j}$, where γ is the gyromagnetic ratio of the nucleus.

2.1 Larmor frequency

Let us consider a system of angular momentum $\boldsymbol{j}$ and magnetic moment $\boldsymbol{m}$ in a static magnetic field $\boldsymbol{H_0}$. The angular momentum law is then given by:

$$\frac{\mathrm{d}\boldsymbol{j}}{\mathrm{d}t} = \boldsymbol{m} \wedge \boldsymbol{H_0} \Longrightarrow \frac{\mathrm{d}\boldsymbol{m}}{\mathrm{d}t} = \gamma \boldsymbol{m} \wedge \boldsymbol{H_0} \tag{1}$$

Taking the scalar product of this equation with $\boldsymbol{m}$ or $\boldsymbol{H_0}$ shows that norm of the magnetic moment as well as the angle between $\boldsymbol{m}$ and $\boldsymbol{H_0}$ are conserved.

Let us arbitrarily decide $\boldsymbol{H_0}$ to be along the z-axis. The projection of equation (1) in the xy-plane is then given by:

$$\frac{\mathrm{d}\boldsymbol{m}_{xy}}{\mathrm{d}t} = \gamma \boldsymbol{m}_{xy} \wedge \boldsymbol{H_0} \Longrightarrow \frac{\mathrm{d}^2\boldsymbol{m}_{xy}}{\mathrm{d}t^2} = -\gamma^2 H_0^2 \boldsymbol{m}_{xy} \tag{2}$$

Equation (2) describes the precession of $\boldsymbol{m}$ about $\boldsymbol{H_0}$ with a frequency $\nu_0 = -\frac{\gamma H_0}{2\pi}$, called the Larmor frequency. The system is illustrated in figure 1.

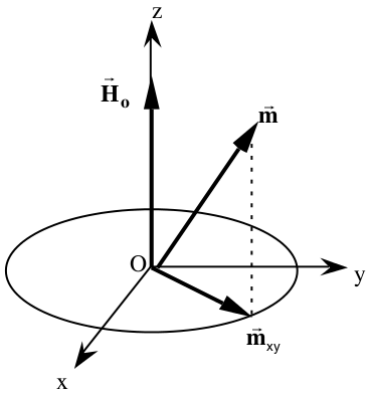

Figure 1: Precession of the magnetic moment about a magnetic field.

2.2 The rotating frame of reference

In the study of NMR, it is helpful to introduce a rotating frame of reference which rotates about $\boldsymbol{H_0}$ in the same direction in which the nuclear moments precess. In our case, we introduce the rotating frame of reference (O, x', y', z') which rotates about $\boldsymbol{H_0}$, i.e. the rotation is represented by the vector $\boldsymbol{\omega} = \omega \hat{\boldsymbol{e}}_z$. The time derivative of $\boldsymbol{m}$ is then given by:

$$\frac{\mathrm{d}\boldsymbol{m}}{\mathrm{d}t} = \frac{\partial \boldsymbol{m}}{\partial t} + \boldsymbol{\omega} \wedge \boldsymbol{m} \tag{3}$$

where the total derivative represents the motion in (O, x, y, z) and the partial derivative the motion in (O, x', y', z'). Plugging (3) into equation (1) yields

$$\frac{\partial \boldsymbol{m}}{\partial t} = \gamma \boldsymbol{m} \wedge \boldsymbol{H}_{\text{eff}} \tag{4}$$

where $\boldsymbol{H}_{\text{eff}} = \boldsymbol{H_0} + \frac{\boldsymbol{\omega}}{\gamma}$. The obtained is of exactly the same form than equation (1), except that the precession is now about $\boldsymbol{H}_{\text{eff}}$ rather than $\boldsymbol{H_0}$.

Let suppose that we apply a field $\boldsymbol{H}_1$ perpendicular to $\boldsymbol{H_0}$ constant in (O, x, y, z), i.e. rotating about $\boldsymbol{H_0}$ with angular frequency ω in the fixed frame of reference. It will shown later on when we discuss the pulse methods that this magnetic field corresponds to a radiofrequency field. The effective magnetic field is now given by

$$\boldsymbol{H}_{\text{eff}} = \left(\boldsymbol{H_0} + \frac{\boldsymbol{\omega}}{\gamma}\right) + \boldsymbol{H_1} \tag{5}$$

By introducing $\omega_1 = -\gamma H_1$, we get:

$$\boldsymbol{H}_{\text{eff}} = \frac{1}{\gamma}[(\omega - \omega_0)\hat{\boldsymbol{e}}_z - \omega_1 \hat{\boldsymbol{e}}_{x'}] \tag{6}$$

$$\tan\theta = \frac{\omega_1}{\omega_0 - \omega} \tag{7}$$

where θ is the angle between $\boldsymbol{H_0}$ and $\boldsymbol{H}_{\text{eff}}$. Equation (6) shows that at resonance, i.e. if the frequency of H_1 is exactly the Larmor frequency, $\boldsymbol{H}_{\text{eff}} = \boldsymbol{H}_1$. This gives the basic idea for all pulse methods: By applying a radiofrequency field at the Larmor frequency during a time τ, it is possible to change the orientation of the magnetic moment by a rotation of angle

$$\theta = \gamma H_1 \tau \tag{8}$$

about the x'-axis (if we arbitrarily assign H_1 along the x'-axis). Once the field $\boldsymbol{H}_1$ is stopped, the system evolve freely towards its equilibrium state, i.e. the magnetic moments will realign with the external field $\boldsymbol{H_0}$.

2.3 Macroscopic generalization: Magnetization and relaxation

In NMR, the studied system is a set of nuclear spins, for which the absorption of energy is the source of information. The transition energy for a single magnetic moment of one nucleus is too small to be detected, which forces to study a large number of nuclear spins (10^{18} or more). To study this system, it is therefore necessary to introduce a macroscopic variable. Under the hypothesis that the nuclear moments $\boldsymbol{m}$ are independent (which is a good approximation for liquids, but not for solids), the variable of interest is the magnetization $\boldsymbol{M}$, given by:

$$\boldsymbol{M} = \sum \boldsymbol{m} \tag{9}$$

where the sum goes over all the nuclear spins of our system. Plugging the magnetization into equation (4) yields

$$\frac{\partial \boldsymbol{M}}{\partial t} = \gamma \boldsymbol{M} \wedge \boldsymbol{H}_{\text{eff}} \tag{10}$$

and using

$$H_{\text{eff,x}'} = H_1 \qquad H_{\text{eff,y}'} = 0 \qquad H_{\text{eff,z}'} = H_0 + \frac{\omega}{\gamma}$$

$$\frac{\partial M_{x'}}{\partial t} = \gamma M_{y'} \left(H_0 + \frac{\omega}{\gamma} \right) \tag{11}$$

$$\frac{\partial M_{y'}}{\partial t} = \gamma \left[M_{z'} H_1 - M_{x'} \left(H_0 + \frac{\omega}{\gamma} \right) \right] \tag{12}$$

$$\frac{\partial M_{z'}}{\partial t} = -\gamma M_{y'} H_1 \tag{13}$$

These equations are incomplete because they don't contain the relaxation, which brings the system back to equilibrium.

At equilibrium, $\boldsymbol{M}$ has no component in x'y'-plane. After the field $\boldsymbol{H_1}$ has been applied, $\boldsymbol{M}$ now has a component along the y'-axis. By exchanging energy with each other, the moments spread out in the plane, causing $M_{y'}$ to decay exponentially with a time constant T_2. Due to the potential inhomogeneities of the static field $\boldsymbol{H_0}$, some magnetic moments will precess slower or faster than others, contributing also to the decay of $M_{y'}$. The overall decay of $M_{y'}$ is therefore exponential with a time constant T_2^*. The relaxation of $M_{y'}$ is called spin-spin relaxation, because it is a result of the interaction between spins.

$M_{z'}$ relaxes through the interaction of the spins with the environment. More specifically, the spins realign with the z'-axis by losing energy to their surroundings. This relaxation is called spin-lattice relaxation and it causes an exponential return of $M_{z'}$ towards its equilibrium value with a time constant T_1. Once $M_{z'}$ has returned to its original value, $M_{y'}$ has to be zero, which implies the following :

$$T_2^* \leqslant T_2 \leqslant T_1 \tag{14}$$

The relaxation phenomenons are illustrated in figure 2.

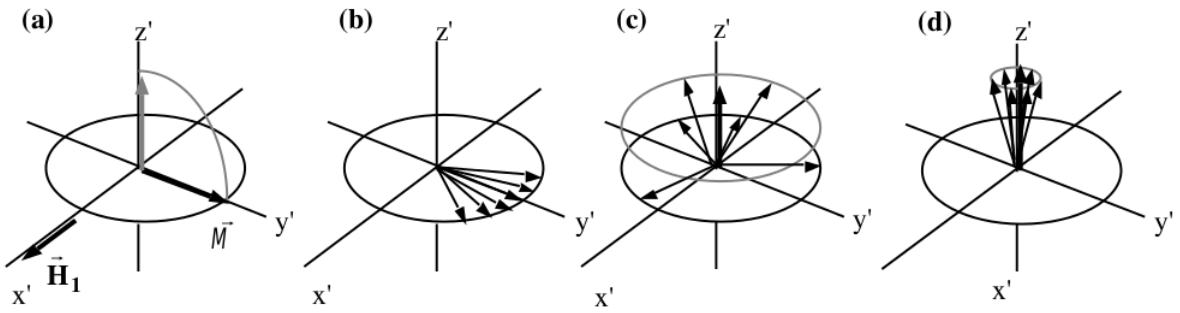

Figure 2: Relaxation phenomenons. (a) Tipping of the magnetization (b) Dephasing of the nuclear moments by spin-spin relaxation and magnetic field inhomogeneities (c) Decay of $M_{y'}$ (d) Return of $M_{z'}$ to equilibrium value

Adapting the above equations to incorporate the relaxation phenomenons yields the Bloch equations:

$$\frac{\partial M_{x'}}{\partial t} = M_{y'} \Delta\omega - \frac{M_{x'}}{T_2} \tag{15}$$

$$\frac{\partial M_{y'}}{\partial t} = (-M_{x'} \Delta\omega - M_{z'} \omega_1) - \frac{M_{y'}}{T_2} \tag{16}$$

$$\frac{\partial M_{z'}}{\partial t} = \omega_1 M_{y'} - \frac{M_{z'} - M_0}{T_1} \tag{17}$$

where $\Delta\omega = \omega - \omega_0$.

3 Experiment Procedure

In this experiment, we will determine the characteristic time constants of the spin-spin and spin-lattice relaxations of a Cu_2SO_4 probe of different concentrations. Furthermore, the concept of MRI will be explored by recreating images of teflon objects in the same chemical environments.

The methods used for measurements are all pulse based, i.e. the system is subjected to a short radiofrequency pulse. This pulse can be approximated by a square wave. Furthermore, the length of the pulse t_p is negligible relative to T_1 and T_2.

3.1 Free Induction Decay and measuring t_{90°

The measurement of the FID is the basic method to determine the magnitude and other properties of the magnetization.

Applying a radiofrequency field during a time t_p to the system changes the orientation of the magnetization by angle $\theta = \gamma H_1 T_p$ (in resonance). The experiment is set up in such a way that the change of orientation of the magnetization induces an electromotive force in a coil whose axis is parallel to the Ox'-axis, therefore measuring the amplitude of $M_{y'}$ as function of time. This signal is called Free Induction Decay (short FID). Free because it occurs after the pulse. Induction because the signal is due to the induction of current in the measurement coil. If the frequency of the radiofrequency field is exactly the Larmor frequency, the obtained signal is an exponential decay illustrated in figure 3.

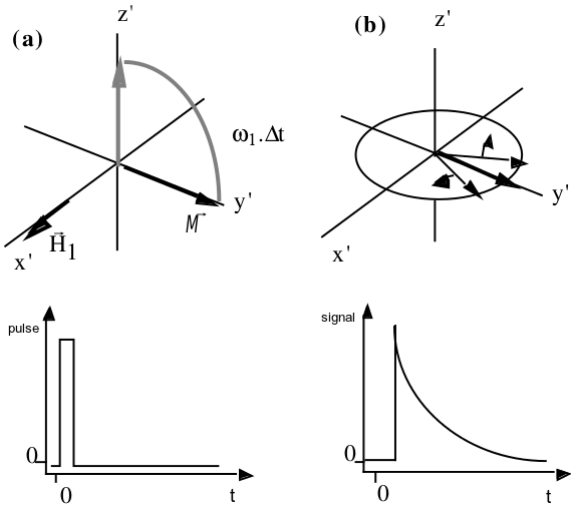

Figure 3: Illustration of the FID principle with a t_{90° pulse.

If the radiofrequency is different from the Larmor frequency, an oscillatory movement is added to the FID because the microscopic nuclei moments will have rotational movement relative to the rotating frame of reference. The resulting "out of resonance" signal is illustrated in figure 4.

The most important pulse which will be used throughout the experiments is the pulse 90°. It means applying the radiofrequency field $\boldsymbol{H_1}$ at the Larmor frequency for a time t_{90° such that the magnetization is rotated by an angle of $\frac{\pi}{2}$. After the pulse, $\boldsymbol{M}$ is therefore parallel to Oy'. The value of t_{90° is determined by varying the length of the pulse and measuring the initial amplitude of the resulting FID. It is easy to see that $M_{y'} = M_0 \sin\theta$. Plotting the initial amplitude as function of the length of pulse therefore yields a sinus. The value for which the FID attains its maximum is given by t_{90°.

3.2 Measuring T_1

The method to measure T_1 is called the $180^\circ, \tau, 90^\circ$ sequence. First, a 180° pulse rotates the magnetization such that $M_{z'}$ is equal to $-M_0$ along the z'-axis. The only process of relaxation is

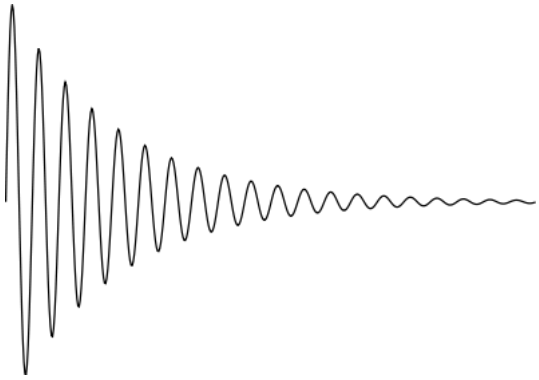

Figure 4: Out of resonance FID.

the lattice-spin relaxation whose time constant is T_1: $M_{z'}$ goes from $-M_0$ back to its equilibrium value. The experiment only measures magnetization along the Oy'-axis. Therefore, by applying a pulse 90° after a time τ the magnetization is rotated onto the Oy'-axis, such that the initial height of the resulting FID is proportional to the value of $M_{z'}$ at time τ. Once the system has returned to equilibrium, the process can be repeated with a different value for τ, thereby yielding the decay curve of $M_{z'}$.

Using Bloch's equation with $M_{z'} = M_{y'} = 0$ and $M_{z'}(t = 0) = -M_0$:

$$\frac{\partial M_{z'}}{\partial t} = -\frac{M_{z'} - M_0}{T_1}$$

gives the solution:

$$M_{z'}(t) = M_0 \left(1 - 2\exp\left(-\frac{t}{T_1}\right)\right) \tag{18}$$

The process is illustrated in figure **??**.

3.3 Measuring T_2

To measure T_2 and not T_2^*, the effects of the inhomogeneity of the magnetic field have to be canceled. A method to do so was first proposed by Hahn, who called it the spin-echo method. The pulse sequence that is applied to the system is $90°, \tau, 180°$. The measurement is then done at a time 2τ. The first pulse tips the magnetization by 90°. Because of the inhomogeneity of the field, the individual microscopic magnetic moments of the nuclei feel different values for H_1, which results in range of precession frequencies centered around the Larmor frequency. After a time τ, a 180° pulse rotates each of the microscopic moments by 180° about the x'-axis, which results in a rephasing of the moments at a time 2τ. The initial height of the resulting FID is then proportional to the relaxed magnetization due to spin-spin interactions after a time 2τ. By varying τ, it is possible to reconstruct the exponential decay of $M_{x'y'}$. $M_{x'y'}$ therefore obeys the following law:

$$M_{x'y'} = M_0 \exp\left(-\frac{2\tau}{T_2}\right) \tag{19}$$

In this experiment, we will consider the effects of molecular diffusion to be negligible.

The process is illustrated in figure **??**.

3.4 Magnetic resonance imagery

Magnetic resonance imagery uses the fact that the Larmor frequency of the nuclei depends on the magnitude of the magnetic field. By applying a gradient to the magnetic field, it is possible to modify the Larmor frequences depending on the position of the nuclei. Furthermore, the intensity of the magnetization is directly related to the density of the sample. By measuring the magnetization

it is therefore possible to determine the density distribution in the sample, thus reconstructing an image.

Since in this experiment it is only possible to have a gradient in a linear direction, to reconstruct a 2D image, several measurements of the sample at different angles are required.

4 Results

4.1 Measurement of t_{90°

Figure 5 shows the amplitude of the obtained signal (proportional to the magnetization) as a function of the pulse duration. The maximum value is theoretically obtained at a pulse duration that shifts the magnetization by 90 °. The obtained pulse duration is therefore given by:

$$\boxed{t_{90^\circ} \approx 10.5\mu\text{s}} \tag{20}$$

According to formula (8), the angle of magnetization is given by $\theta = \tau\gamma H_1$. The error on the angle may therefore be computed by:

$$\Delta\theta = \left|\frac{\partial\theta}{\partial\tau}\right|\Delta\tau + \left|\frac{\partial\theta}{\partial\gamma}\right|\Delta\gamma + \left|\frac{\partial\theta}{\partial H_1}\right|\Delta H_1 \tag{21}$$

However, knowing that γ is a constant and assuming the error on H_1 to be negligible, the error on the angle is simplified to

$$\Delta\theta = \frac{\Delta\tau}{\tau}\theta \tag{22}$$

Finally, the NMR control software had an uncertainty of 0.5μs on the pulse duration. Therefore the estimated error on the angle is given by

$$\boxed{\Delta\theta = \frac{0.5}{10.5}\frac{\pi}{2} \approx 0.0748 \approx 4.28^\circ} \tag{23}$$

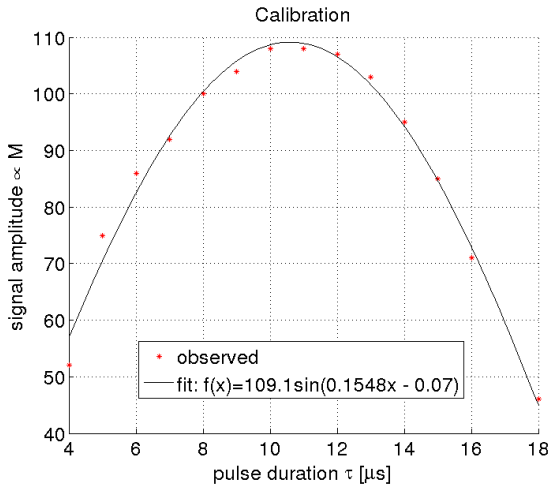

Figure 5: Measuring t_{90°: signal amplitude as a function of pulse duration.

4.2 Measurement of T_1

The results obtained in order to calculate T_1 are illustrated in figure 6. 6(a) shows a signal proportional to the magnetization M as a function of the wait time τ, described in section 3.2. Knowing that the magnetization is proportional to the sinus of the spin angles, the error on it

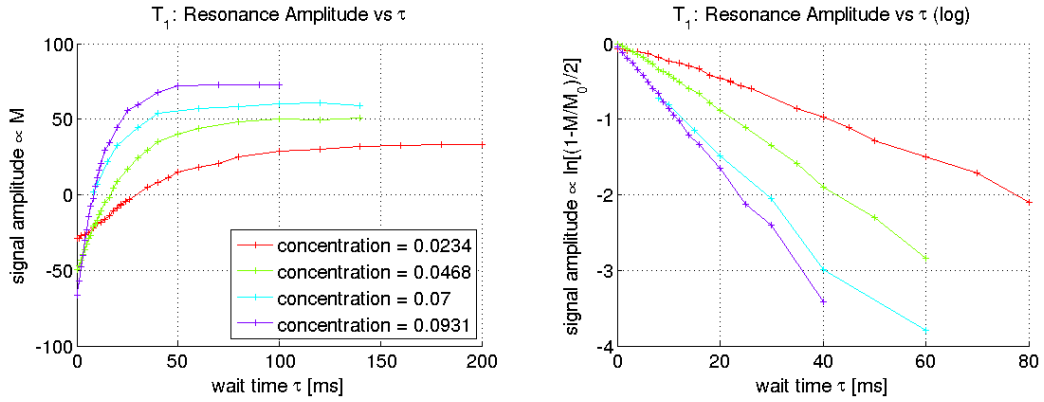

(a) (b)

Figure 6: Data obtained for determining T_1. (a) Shows the signal amplitude (proportional to magnetization) as a function of the time τ. (b) Shows the signal amplitude (M) transformed by $ln((1 - M/M_0)/2)$.

would also be proportional to the error on the 90° pulse-angle. However, the proportionality factor between the measured amplitude and and the magnetization is unknown, therefore it is senseless to plot any error on the obtained data.

Nevertheless, it can be seen that the curves obtained resemble an exponential as described by equation (18). Rearranging this equation yields a linear equation in time:

$$\frac{-1}{T_1}t = \ln\left[\frac{1}{2}(1 - \frac{M}{M_0})\right] \tag{24}$$

The right-hand-side of the previous equation is applied to the measured signal, yielding linear curves as shown in figure 6(b). Note that the slopes of these curves represent $-1/T_1$, which will be discussed later on.

4.3 Measurement of T_2

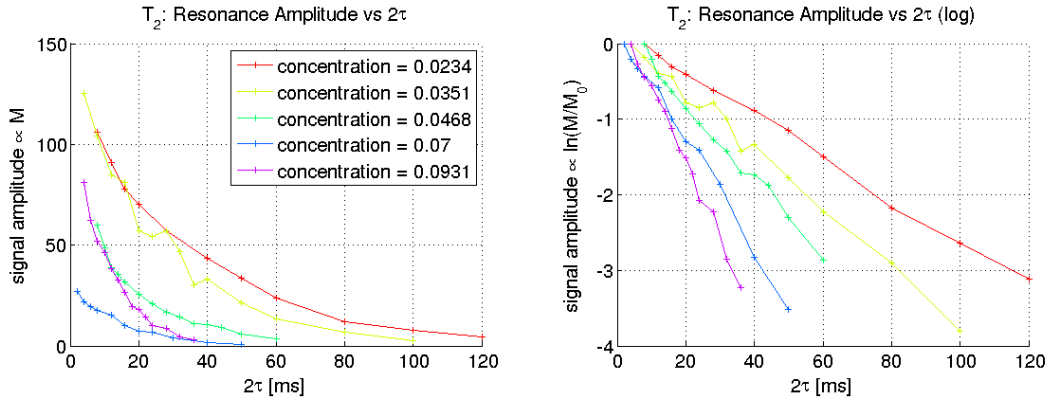

(a) (b)

Figure 7: Data obtained for determining T_2. (a) Shows the signal amplitude (proportional to magnetization) as a function of the time 2τ, described in section 3.3. (b) Shows the signal amplitude (M) transformed by $ln(M/M_0)$.

Figure 7 shows the data obtained to measure the spin-spin relaxation time T_2. It can clearly be seen that the data obtained in 7(a) forms an exponential and is coherent with equation (19).

Unfortunately, due to the same reasons described in the previous section no errors may be calculated on this graph.

However, the data may be rearranged to represent the equation

$$\frac{-1}{T_2}t = \ln\left[M/M_0\right] \tag{25}$$

This is performed in figure 7(b), therefore the slopes represent $-1/T_2$. The values obtained for the slopes will be discussed in the next section.

4.4 Relation between concentration and characteristic time constants

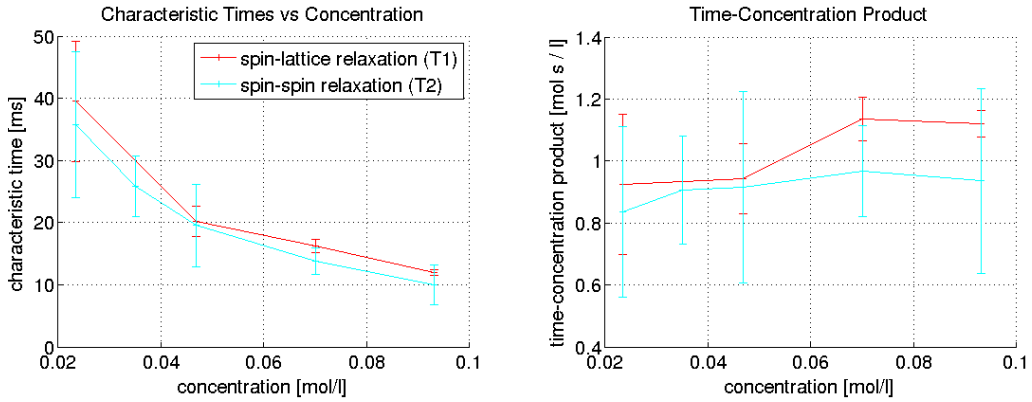

(a) (b)

Figure 8: (a) Characteristic times T_1 and T_2 as a function of the probes concentration. (b) Product of concentration and characteristic time.

Considering the results obtained in the two previous sections, the characteristic times T_1 and T_2 may be computed by taking the negative inverse of the slopes of figures 6(b) and 7(b). For every concentration tested, the obtained values are plotted in figure 8(a).

The errors are obtained with the following procedure. First, the equations (18) and (19) may be written as

$$T_1 = -t/\ln\left[\frac{1}{2}(1-\frac{M}{M_0})\right] \tag{26}$$

and

$$T_2 = -t/\ln\left[M/M_0\right] \tag{27}$$

respectively. Second, the value M_0 is computed for each of the equations. In the case of T_1, this is done by taking the mean value of the last amplitudes measured in 6(a). In the case of T_2, M_0 is computed by taking the first amplitudes in 7(a)[1]. Third, values for T_1 and T_2 are calculated by replacing M and t in the above equations with observed values. Finally, the error is given by the standard deviation of these values.

4.5 Magnetic resonance imagery

Two shapes of probes were examined: a cross and a spiral. The reconstructed images are shown in figure 9.

[1] a discussion on this method is proposed in the section "Discussion"

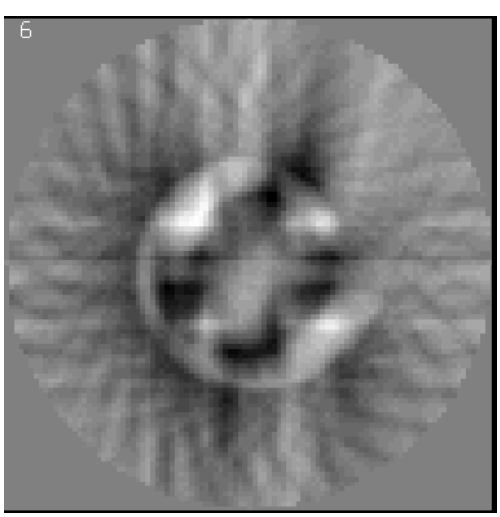

(a) cross

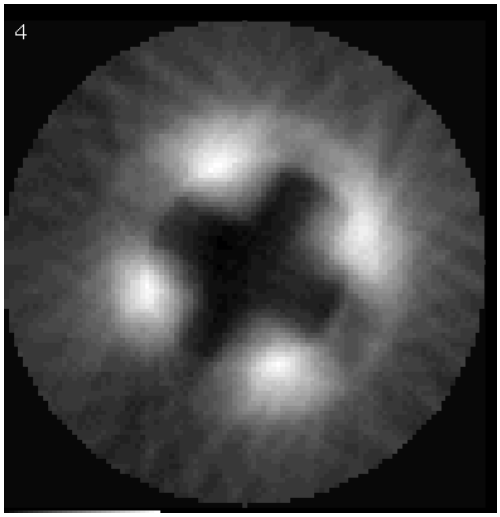

(b) cross

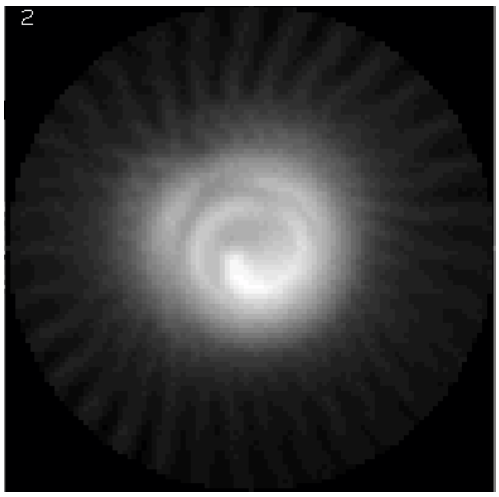

(c) spiral

Figure 9: Images of samples obtained using NMR. Sample in (a) and (b): cross. Sample in (c): spiral.

5 Discussion

5.1 Relation between concentration and characteristic time constants

In the light of the results obtained, a first observation is that the characteristic time constants both obey the exponential laws given in theory. Furthermore, as given in equation (14), the obtained time constants verify $T_2 \leq T_1$ for every concentration.

It can be seen that the obtained curves relating characteristic times to concentrations vaguely resemble a hyperbola. Furthermore, the product of characteristic time and concentration is constant within the margin of error and close to one (this is shown on figure 8(b)). This leads to an empirical law relating characteristic time constant and concentration:

$$T_x C = A_x \Longrightarrow \boxed{C = \frac{A_x}{T_x}} \tag{28}$$

where

- T_x is a characteristic time constant ($x = 1$ or 2)

- A_x is the constant obtained in graphic 8(b)
- C is the concentration of the Cu_2SO_4 solution

However, to confirm this law more measurements of different concentrations would be required and margins of error should be reduced.

Considering the error margins, it can be seen that they are considerably larger for T_2 than for T_1. This is related to the way the error was determined, more precisely to the value of M_0. In case of T_1, the law is an exponential that converges to M_0, therefore a good approximation of M_0 is given by taking an average of the last (constant-looking) points. However, in the case of T_2 the law does not converge to M_0 but rather passes M_0 at time zero. Achieving a measurement of a zero length time is impossible and small values are very hard to achieve since high precision instrumentation is required. Therefore, taking the first data point as a value for M_0 is less precise and yields larger error margins.

Nevertheless, the obtained data illustrate a possible application of NMR, namely the determination of an unknown substance as is done in spectroscopy.

5.2 Magnetic resonance imagery

The examined probes' geometry is clearly visible in the reconstructed images. It can be noted that dark areas of the image correspond to areas whose interactions were less with NMR. The light areas correspond to areas in which the Cu_2SO_4 solution was present. As an example, it can be seen in the a droplet of solution was present on top of the cross on image (a) (as we later discovered examining the probe, this was truly the case!). Unfortunately, the images came out a bit small (even though the width of our FID seemed adequate, see figure 10 in appendix) and changes in the acquisition parameters would have to be applied in order to obtain a greater zoom.

Nevertheless, the obtained images show the possibilities of magnetic resonance imagery such as used in medical applications.

6 Conclusion

This report demonstrated the concept of nuclear magnetic resonance. Specific time constants were measured for a probe of Cu_2SO_4 of different concentrations and an empirical law was determined, thus illustrating the determination of substances through NMR. Furthermore, NMR was used in the context of magnetic resonance imagery to produce images of different probes.

Although the results were accompanied with significant error margins, the goal of this report has been achieved and the wide application possibilities of NMR have been shown.

References

[1] P. Scherrer, *Resonance Magnetique Nucleaire*. EPFL, March 1998.

List of Figures

A Appendix

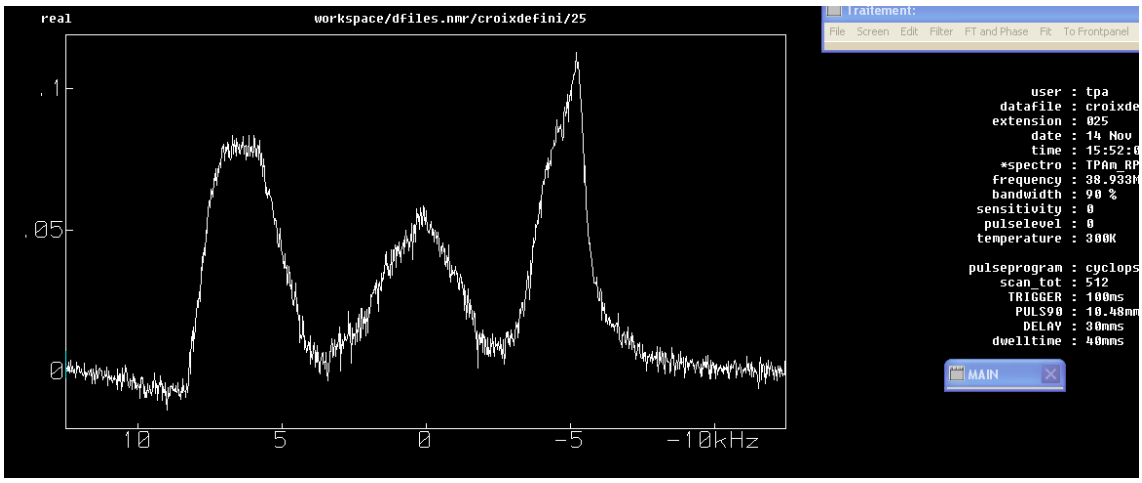

Figure 10: Example of obtained FID for MRI.